13

Optimization of fabrication processes for Nb, NbN, NbTiN films and high-quality tunnel junctions for terahertz receiving circuits.

© A.M. Chekushkin,[1] L.V. Filippenko,[1] A.A. Lomov,[2] Dong Liu,[3] Sheng-Cai Shi,[3] V.P. Koshelets[1]

[1] Kotelnikov Institute of Radio Engineering and Electronics,
125009 Moscow, Russia
[2] Valiev Institute of Physics and Technology, Russian Academy of Sciences,
117218 Moscow, Russia
[3] Purple Mountain Observatory, CAS, 2 West Beijing Rd,
210008 Nanjing, China
e-mail: chekushkin@hitech.cplire.ru

Received May 11, 2021
Revised May 11, 2021
Accepted May 11, 2021

This paper describes the optimization of the existing technology for the fabrication of superconducting films and high-quality tunnel junctions on a magnetron sputtering facility. To expand the frequency range to 1.1 THz and to obtain the limiting parameters of superconducting elements, the regimes of production of Nb, NbN, NbTiN films were optimized. These films are used to fabricate superconductor-insulator-superconductor Nb/Al–AlN/NbN tunnel junctions. Al and NbTiN films are required to create receiving elements at frequencies above 700 GHz (the cutoff frequency for niobium); such structures are being developed for the radio astronomy array receiver located in the Atacama Pathfinder Experiment telescope.

Keywords: superconductivity, tunnel junctions, magnetron sputtering, thin films.

DOI: 10.21883/TP.2022.13.52234.135-21

Introduction

Superconductor–insulator–superconductor (SIS) tunnel junctions based on niobium are the main elements of ultrasensitive receivers for radioastronomy [1,2]. The adjusting structures of materials with high limiting frequency, such as NbTiN, are used to increase the operating frequency of the receivers above 700 GHz (the gap frequency of niobium) [3–5].

Niobium is a good getter, therefore niobium-based films are usually deposited using magnetron in high deposition rate modes to prevent from contamination with residual gases. For niobium films, made using DC magnetron with diameter of 76.2 mm at high power (1000−1500 W), the high deposition rate (up to 2 nm/s) is possible even at significant distance of sample from target (up to 120 mm). With such approach the high quality films were made (NbN: $\rho = 140-230\,\mu\Omega\cdot$cm, resistance ratio $R(300\,\mathrm{K})/R(20\,\mathrm{K})$ (then $R_{300}/R_{20}) = 0.8-0.9$, T_c on silicon substrate 14−15 K). It should be noted that NbN and NbTiN films were made without additional heating of substrates; heating to 400−500°C allows to achieve the higher T_c of about 16−16.5 K. However, for manufacturing the integral structures based on SIS junctions using lift-off method this approach can not be used due to presence of a resistive mask, that is hardened at temperature above 150°C.

During fabrication of Nb, NbN, NbTiN films in the mode with DC magnetron high power (up to 1500 W) the technical problems, related to high power densities at the magnetron (up to 34 W/cm^2), were observed: target overheating, strong sputtering of restrictive screens and arching. When these problems appeared directly during films deposition, the results were unrepeatable and unpredictable. In this study we present the results of the optimization of niobium and its compounds films deposition modes using magnetron sputtering; the data of X-ray diffraction studies of phase composition and texture features of NbTiN films (sect. 1). In sect. 2 the methods of forming the tunnel SIS structures based on niobium, intended for terahertz receiving devices, are described.

1. Optimization of films manufacturing modes

DC magnetron power was lowered to 500 W to reduce the thermal load on target and improve reproducibility of the films parameters. High-purity niobium targets (99.95%) were used for Nb and NbN films fabricating. Target with ratio of Nb:Ti = 78:22 was used for NbTiN films fabricating. The distance between target and sample was reduced to 50 mm to maintain the deposition rate at a level of 1−2 nm/s. Gas (Ar) pressure varied in a chamber for searching the optimum modes of Nb films fabricating. Mixture of Ar and N_2 gases was used for NbN and NbTiN films fabricating, therefore, beside variation of the general pressure of the gases mixture, their proportion was also changed. The characteristic value of preliminary vacuum in the unit was $5-8\cdot10^{-8}$ mbar. All samples were made on silicon substrates with buffer layer of Al_2O_3 with thickness

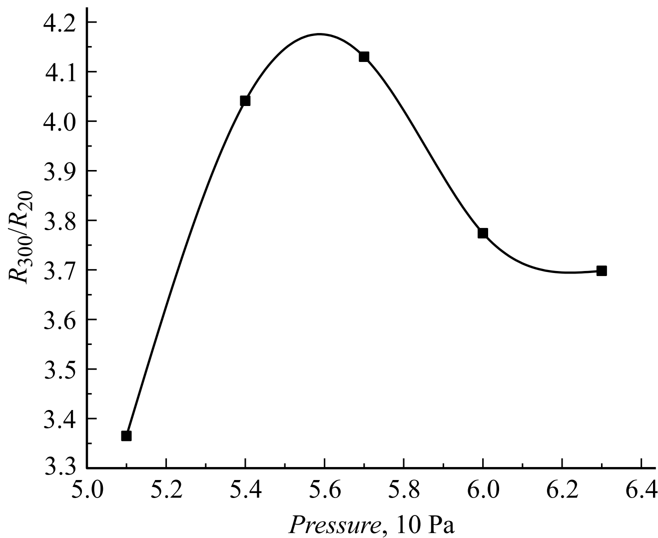

Figure 1. Dependence of resistance ratio R_{300}/R_{20} on Ar pressure.

of 100 nm. Manufactured films thickness was from 200 to 400 nm.

Nb films fabricating conditions were optimized. Specific resistivity of the films at room temperature was used as a control parameter, along with the resistance ratio R_{300}/R_{20}, that for high-quality Nb films, made by magnetron sputtering, is about 4. At first the DC magnetron power was changed from 1000 to 400 W with a step of 100 W, and then the distance between sample and target was changed (from 120 to 50 mm). The final parameter was argon pressure during the film deposition. Fig. 1 shows the dependence R_{300}/R_{20} on Ar pressure for $P = 500$ W, the distance between target and sample is 50 mm, films thickness is about 260 nm, deposition rate is about 15 A/c, $T_c = 9.23$ K.

Samples of NbN films were made at lower magnetron power of 500 W at various parameters of pressure, gas proportions and distance between target and magnetron. Selection of parameters of NbN films deposition was performed as per the algorithm, similar to Nb films, considering adding of the another parameter — argon and nitrogen gases proportion. For NbN films, made at magnetron power of 500 W, proportions of $Ar/N_2 = 6.7$ and general pressure of $7.2 \cdot 10^{-1}$ Pa the following parameters were observed: $\rho = 180\,\mu\Omega$·cm, $R_{300}/R_{20} = 0.9$, T_c on silicon substrate was 14.7 K. Process of optimization of NbN film formation modes is not completed yet; but the already observed parameters allow to use these films in manufacturing of the high-quality SIS junctions based on Nb–AlN–NbN.

For high-frequency signal receiving the SIS mixers are integrated into a microstrip line, consisting of 325 nm NbTiN as a bottom electrode, thick layer of Al (450 nm) as a top conductor, divided with 250 nm SiO_2. For implementation of the terahertz receiving systems the losses in this line should be minimized; therefore the following parameters of NbTiN films are required: resistivity of 90–110 $\mu\Omega$·cm, critical temperature of 14.5–15.2 K, thickness of 325 nm. Such parameters as pressure, gas proportions, distance between target and sample were optimized. Fig. 2 shows the dependencies of the resistivity and critical temperature on nitrogen flow (N_2) at the magnetron constant power of 500 W, distance between sample and target of 60 mm and constant Ar flow of 40 sccm. Pressure range in gas mixture is from $5.2 \cdot 10^{-2}$ Pa to $6 \cdot 10^{-1}$ Pa.

Dependence of resistivity and critical temperature of NbTiN on pressure at constant gas proportion of $Ar/N_2 = 6.67$ was also studied (Fig. 3).

NbTiN films, made at increased magnetron power (1500 W), had a semiconducting nature of dependence of resistivity on temperature, while the samples, made at lowered magnetron power (500 W), had a metallic nature of dependence, with plateau reaching at about 60 K (Fig. 4).

NbTiN films, being the base layer for the further study of three-layer SIS structure, should have not just a low resistivity and high T_c, but the low-roughness surface also. Also, the physical and chemical properties of the films

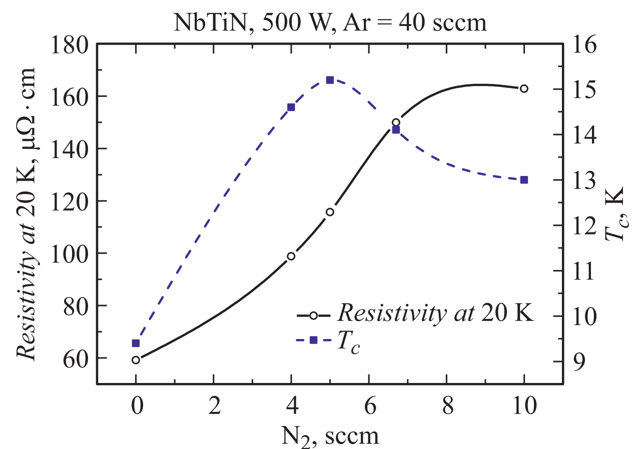

Figure 2. Dependence of resistivity and critical temperature of NbTiN on nitrogen flow in gas mixture.

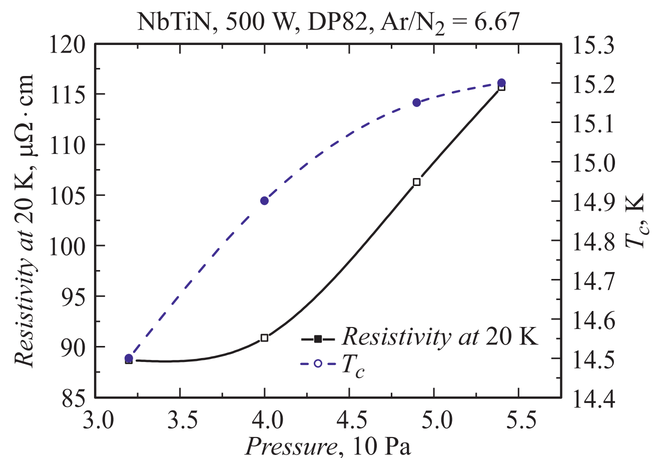

Figure 3. Dependence of resistivity at 20 K and critical temperature of NbTiN on Ar/N_2 mixture pressure.

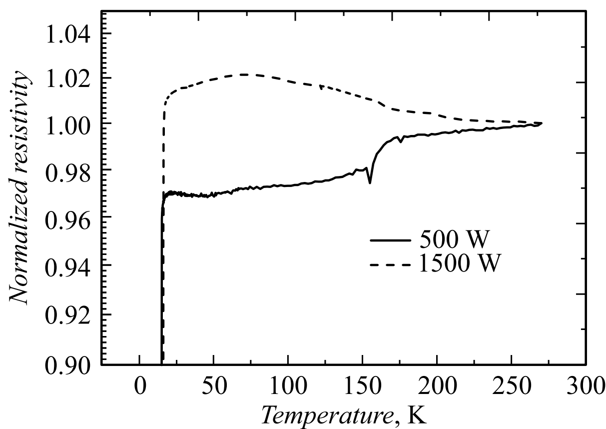

Figure 4. Dependence of resistivity on temperature for NbTiN films, made at various magnetron power.

depend on their phase composition, morphology, crystallites distribution in terms of orientation and dimensions.

X-ray diffraction studies of the phase composition and texture features of NbTiN films with various resistivity and T_c: $\rho = 102\,\mu\Omega\cdot$cm, $T_c = 14.7$ K and $\rho = 256\,\mu\Omega\cdot$cm, $T_c = 14$ K were performed. The significant difference in the films fabricating mode was the operating pressure, as well as proportion of gases: argon and nitrogen. Low-resistivity film was made at pressure of $5.3 \cdot 10^{-1}$ Pa, $Ar/N_2 = 10$ (sample T1-2), high-resistivity film — at pressure of $7.9 \cdot 10^{-1}$ Pa, $Ar/N_2 = 5.6$ (sample T1-3). X-ray diffraction studies of the phase composition and microstructure features of the grown NbTiN-based films were performed at SmartLab diffractometer, equipped with the rotating copper 9 kW anode and parabolic G'bel mirror. X-ray diffractograms of the studied films were taken in the parallel beam geometry with grazing angle of 1° (off-plain geometry). Radiation, reflected from the sample, was registered during scanning with a detector with the Soller slit of 0.114° installed in front of its window.

X-ray diffractograms of the studied films T1-2 and T1-3 are presented in Fig. 5. It can be observed that number of diffraction peaks is the same, and their angular positions almost coincide. Peak at the angle $2\Theta = 56.12(°)$ corresponds to asymmetrical 113 reflection from substrate of Si(001). The observed diffraction peaks from films T1-2 and T1-3 are in coincidence with a database of PDF-2 card №01-077-2990. Fig. 5, *a* shows that the peaks from film T1-2 at angles $2\Theta = 35.87, 41.62, 60.42, 72.20$ and $76.04(°)$ coincide with reflections from crystal planes of (111), (200), (220), (113), (222), respectively.

There were no peaks observed in the selected angular range. This result shows that the film T1-2 belongs to niobium titanate nitride of cubic crystal system and spatial group of Fm-3m (225) with crystal grating parameters of $a = b = c = 4.328$ nm, $\alpha = \beta = \gamma = 90(°)$. Comparing the ratios of peaks intensities of the diffractogram with data from card №01-077-2990, it can be observed, that the film T1-2, grown at magnetron power of 500 W, in terms of stoichiometry belongs to $NbTiN_2$ phase, while the exact angular match of diffraction peaks with the database indicates the lack of significant stresses in it.

Analysis of the diffractogram of the film T1-3 (Fig. 5, *b*) shows that the relative peaks intensities significantly differ from the corresponding values, observed for the sample T1-2. Thus, for instance, while for the sample T1-2 peaks intensities $I(111)$ and $I(200)$ are almost equal, they differ for the sample T1-3 by a factor of almost 40. Also, angular positions of all peaks for the film T1-3 are shifted toward lower reflection angles, that corresponds with the increased parameters of the crystal grating by $\Delta a/a \sim 5 \cdot 10^{-3}$. This means that the films composition is different. It seems that in the film, grown at increased pressure, the atomic re-arrangement happened in the grating nodes, thus resulting in their partial absence, for instance, nitrogen atoms. For the more precise interpretation the additional studies using complementary methods are required. Crystallites

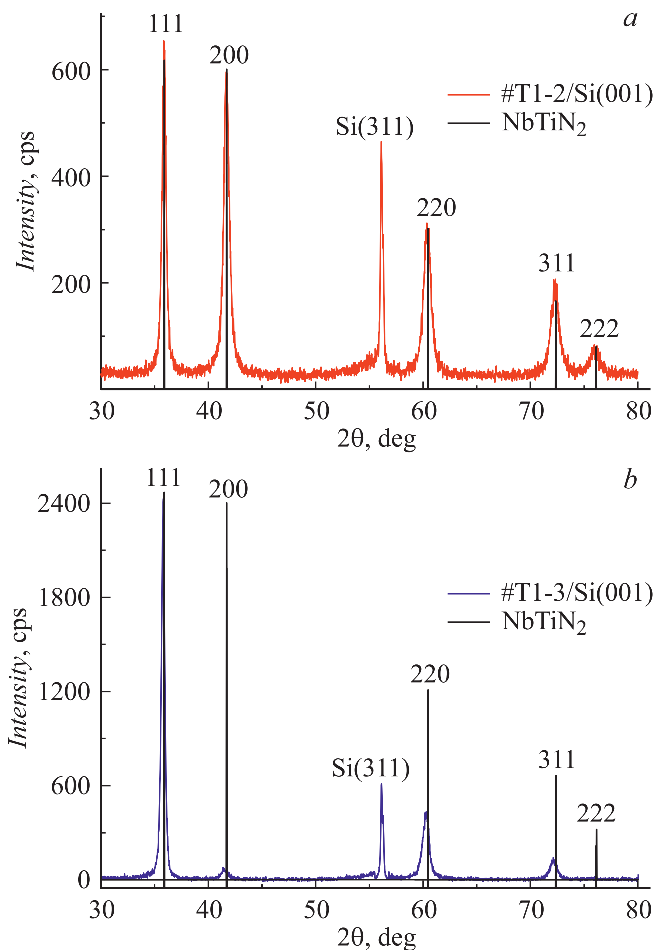

Figure 5. X-ray diffractograms of low-resistivity film T1-2 (*a*), high-resistivity film T1-3 (*b*), grown on substrates of Si(001), and values of intensity and diffraction peaks angular positions for $NbTiN_2$ (PDF card №01-077-2990). Off-plain geometry. Angle of radiation incidence to sample surface is 1°. Cu$K\alpha$-radiation.

dimensions and texture present in film also make influence on relative intensity of the peaks.

To define the crystallites dimensions D from the diffraction peaks broadening the Scherrer formula was used [6]:

$$D = K\lambda/\beta\cos\Theta, \quad (1)$$

where $\lambda = 1.540$ nm is radiation wave length of Cu $K\alpha$, β is diffraction peak full width at half maximum (FWHM), Θ is Bragg angle, K is Scherrer constant, depending on the shape and reflection indices. In our evaluations we used $K = 0.9$.

Analysis of the observed peaks (Fig. 5) shows that their angular width does not depend on the films deposition modes, but depends on the reflection order only. Defined as per formula (1) the dimensions of the crystallites, meeting the conditions for 111 reflection, are the biggest and equal to 22(1) nm. The remaining reflections are made by smaller crystallites with dimensions from 12 to 15 nm.

It follows that, first of all, the films surface roughness will be defined by the larger crystallites, presumably restricted with planes of 111. Secondly, the surface roughness will be higher for the film T1-3, with the clear-cut texture, that exhibits in more intensive 111 reflection and „decreased“ or zero reflection from other crystal planes.

2. Fabrication and study of SIS junctions

Tunnel junctions Nb–AlO_x–Nb [7,8] are the main elements of the majority of modern superconductive electronic devices. Based on modified mode of Nb films fabricating the SIS junctions of Nb–AlO_x–Nb were implemented. Three-layer structure was made in a single vacuum cycle. Thickness of the bottom niobium layer was 2000 A, then the deposition of 7 nm of aluminum was performed, which later was oxidized at pressure of 100 Pa within 20 min, and after that the top niobium layer with thickness of 800 A was deposited. SIS junction of the required area is formed using resistive mask, over which the reactive ion etching in CF_4 gas is performed in the top layer (Nb). Then the anodization of SIS junction faces in electrolyte solution is performed to prevent from micro short circuits. During the following vacuum cycle of deposition the contact layer (top electrode) — aluminum with thickness of 350 nm, is formed over the new resistive mask.

I-V curves of the made SIS junctions were measured at $T = 4.2$ K and the following characteristics were observed: energy gap in superconductor $V_g = 2.78$–2.8 mV, ratio of sub-gap resistance to normal resistance R_j/R_n — up to 30 for R_nS (product of the normal resistance of SIS junction above the gap by its area) — about $120\,\Omega\cdot\mu\text{m}^2$. Fig. 6 shows I-V curve of one of the SIS junctions with area of $15\,\mu\text{m}^2$. Measurements were performed in voltage setting mode using IRTECON software [9], that allows to define the required parameters in automatic mode.

To expand the frequency range to the high frequencies area (atmospheric transmission bands of 790–950 GHz and 950–1150 GHz) the SIS mixers based on three-layer structure of Nb/AlN/NbN with high density of critical current ($30\,\text{kA/cm}^2$) will be used [10–12]. Application of barrier of aluminum nitride is caused by the fact that it is not possible to create a reliable tunneling barrier of aluminum oxide with current density of more than 10–$15\,\text{kA/cm}^2$ [13]. This restriction is related to the fact that during thin AlO_x layer forming by means of aluminum oxidation it is highly possible that this barrier will be not sufficiently uniform over SIS junction area, thus resulting to its rupture and degradation of the tunnel junction [14]. At the same time, the application of niobium nitride in SIS junction allows to use the mixer, based on it, at higher frequencies (up to 1.2 THz). For SIS mixer based on Nb–AlO_x–Nb this frequency is 700–750 GHz.

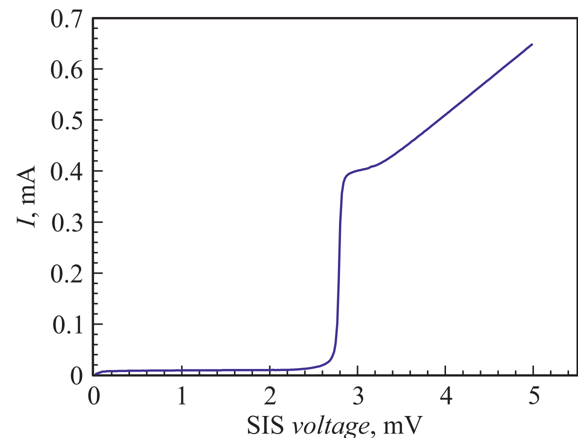

Figure 6. I-V curve of SIS junction of Nb–AlO_x–Nb, made at reduced power of Nb deposition: $V_g = 2.8$ mV, $R_j/R_n = 30$, $R_nS = 120\,\Omega\cdot\mu\text{m}^2$.

Based on modified recipes for Nb and NbN the test structures of Nb–AlN–NbN were made. Three-layer structure was formed within a single vacuum cycle: thin layer of aluminum with thickness of 5–7 nm is applied to the bottom niobium electrode with thickness of 2000 A using magnetron sputtering method. Then, this layer is nitridated in pure nitrogen plasma, while obtaining the required thickness of the tunneling barrier is possible by means of varying the discharge power and nitridation time. Low discharge power and high distance from target to sample allowed to prevent both the tunneling barrier damage with high-energy ions and the additional deposition of target material (Al) during nitration. SIS junction of the required area is formed the same way as in case of Nb–AlO_x–Nb, described above.

The formed structures measurements were performed at $T = 4.2$ K and the following parameters were observed: energy gap in superconductor $V_g = 3.48$–3.51 mV, ratio of sub-gap resistance to normal resistance R_j/R_n up to 28 for R_nS — about $25\,\Omega\cdot\mu\text{m}^2$. I-V curve of one of such junctions is presented in Fig. 7.

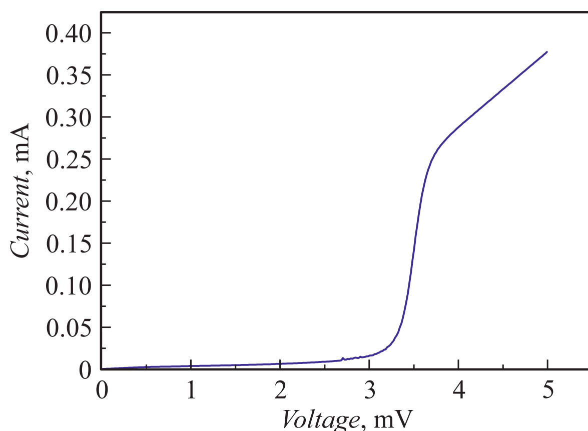

Figure 7. I-V curve of SIS junction of Nb–AlN–NbN with the following characteristics: $V_g = 3.48\,\text{mV}$, $R_j/R_n = 28$, $R_nS = 25\,\Omega\cdot\mu\text{m}^2$.

Conclusion

Optimization of Nb, NbN and NbTiN films fabrication parameters was performed and their characteristics were measured. Test SIS structures of Nb/AlO_x/Nb and Nb/AlN/NbN were fabricated as per the modified technology related to necessity of DC magnetrons operating power decrease. The observed characteristics of tunnel structures ($V_g = 2.78\ldots2.81\,\text{mV}$, R_j/R_n - up to 30 and $V_g = 3.48\ldots3.51\,\text{mV}$, R_j/R_n - up to 28, respectively) indicate the high quality of niobium and niobium nitride films.

Comprehensive study of NbTiN films characteristics was performed at magnetron power lowering to 500 W: at various pressure, distance between sample and target, various proportions of nitrogen and argon gases. It was demonstrated that it is possible to make NbTiN films with characteristic parameters of specific resistivity of $90-110\,\mu\Omega\cdot\text{cm}$ and $T_c = 14.5-15.2\,\text{K}$, that allows to use them during fabrication of the terahertz range receiving elements.

Funding

The study was supported by the Russian Foundation for Basic Research project N 19-52-80023 BRIKS_t. Samples preparation was performed using the unique scientific unit 352529 under the Government Task of the Kotelnikov Institute of Radio Engineering and Electronics of the Russian Academy of Sciences. X-ray diffraction studies of the phase composition, performed by A.A. Lomov, were done under the Government Task of Valiev Institute of Physics and Technology of the Russian Academy of Sciences on the subject N 0066-2019-0004.

Conflict of interest

The authors declare that they have no conflict of interest.

References

[1] A.R. Kerr, S.K. Pan, S.M.X. Claude, P. Dindo, A.W. Lichtenberger, J.E. Effand, E.F. Lauria. IEEE Trans. Terahertz Sci. Technol., **4** (2), 201 (2014). DOI: 10.1109/TTHZ.2014.2302537.

[2] A.M. Baryshev, R. Hesper, F.P. Mena, T.M. Klapwijk, M.R. Hogerheijde, B.D. Jackson, J. Adema, G.J. Gerlofsma, M.E. Bekema, J. Barkhof, L.H.R. de Haan-Stijkel, M. van den Bemt, A. Koops, K. Keizer, C. Pieters, J. Koops van het Jagt, H.H.A. Schaeffer, T. Zijlstra, M. Kroug, C.F. Lodewijk, K. Wielinga, W. Boland, M.W.M. de Graauw, E.F. van Dishoeck, H. Jager, W. Wild. Astron. Astrophys., **577**, A129 (2015). DOI: 10.1051/0004-6361/201425529

[3] B.D. Jackson, G. de Lange, T. Zijlstra, M. Kroug, T.M. Klapwijk. J. Appl. Phys., **97**, 113904 (2005). DOI: 10.1063/1.1927281

[4] B.D. Jackson, G. de Lange, T. Zijlstra, M. Kroug, J.W. Kooi, J.A. Stern, T.M. Klapwijk. IEEE Trans. Microw. Theory Techn., **54** (2), 547 (2006). DOI: 10.1109/TMTT.2005.862717

[5] Y. Uzawa, M. Kroug, T. Kojima, K. Makise, A. Gonzalez, S. Saito, Y. Fujii, K. Kaneko, H. Terai, Z. Wang. IEEE Trans. Appl. Supercond., **27** (4), 500705 (2017). DOI: 10.1109/TASC.2016.2632628

[6] J.I. Langford, A.J.C. Wilson, J. Scherrer. Appl. Cryst., **11** (2), 102 (1978). DOI: 10.1107/S0021889878012844

[7] A.B. Ermakov, S.V. Shitov, A.M. Baryshev, V.P. Koshelets, W. Luinge. IEEE Transact. Appl. Superconduct., **11** (1), 840 (2001). DOI: 10.1109/77.919475

[8] H. A.Huggins, M. Gurwitch. J. Appl. Phys., **57**, 2103 (1983). DOI: 10.1063/1.334403

[9] S. Morohashi, F. Shinoki, A. Shoji, M. Aoyagi, H. Hayakawa. Appl. Phys. Lett., **46**, 2103 (1985). DOI: 10.1063/1.95696

[10] P.N. Dmitriev, I.L. Lapitskaya, L.V. Filippenko, A.B. Ermakov, S.V. Shitov, G.V. Prokopenko, S.A. Kovtonyuk, V.P. Koshelets. IEEE Trans. Appl. Supercond., **13** (2), 107 (2003). DOI: 10.1109/TASC.2003.813657

[11] M.Yu. Torgashin, V.P. Koshelets, P.N. Dmitriev, A.B. Ermakov, L.V. Filippenko, P.A. Yagoubov. IEEE Trans. Appl. Supercond., **17** (2), 379 (2007). DOI: 10.1109/TASC.2007.898624

[12] A. Khudchenko, A.M. Baryshev, K. Rudakov, P.N. Dmitriev, R. Hesper, L. de Jong, V.P. Koshelets. IEEE Trans. on THz Sci. Technol., **6** (1), 127 (2016). DOI: 10.1109/TTHZ.2015.2504783

[13] B. Bumble, H.G. LeDuc, J. Stern. Proc. of the 9th Int. Symp. on Space THz Technol., CIT, PC, 295, (1998).

[14] A.W. Kleinsasser, R.E. Miller, W.H. Mallison, G.B. Arnold. Phys. Rev. Lett., **72** (11), 1738 (1994). DOI: 10.1103/PhysRevLett.72.1738